International Journal of Pharmaceutics 534 (2017) 316–324

Contents lists available at ScienceDirect

International Journal of Pharmaceutics

journal homepage: www.elsevier.com/locate/ijpharm

Research Paper

Physicochemical properties of inclusion complexes of highly soluble β-cyclodextrins with highly hydrophobic testosterone propionate

Christian Celia[a,b], Angela Scala[c], Rosanna Stancanelli[c], Emanuela Surdo[c], Donatella Paolino[d,e], Alessandro Grattoni[b], Nicola Micale[c], Vincenza Crupi[f], Domenico Majolino[f], Massimo Fresta[e,g], Silvana Tommasini[c], Valentina Venuti[f,*], Cinzia Anna Ventura[c,*]

[a] Department of Pharmacy, University of Chieti – Pescara "G. d'Annunzio", Via dei Vestini 31, I-66100 Chieti, Italy
[b] Department of Nanomedicine, Houston Methodist Research Institute, 6670 Bertner Avenue, Houston, TX 77030, USA
[c] Department of Chemical, Biological, Pharmaceutical and Environmental Sciences, University of Messina, Viale Ferdinando Stagno D'Alcontres 31, I-98166 Messina, Italy
[d] Department of Experimental and Clinical Medicine, University of Catanzaro "Magna Græcia", Campus Universitario "S. Venuta", Viale S. Venuta, Germaneto, I-88100 Catanzaro, Italy
[e] IRC-FSH-Interregional Research Center for Food Safety & Health, University of Catanzaro "Magna Græcia", Building of BioSciences, V.le Europa, Germaneto, I-88100 Catanzaro, (CZ), Italy
[f] Department of Mathematical and Computer Sciences, Physical Sciences and Earth Sciences, University of Messina, Viale Ferdinando Stagno D'Alcontres 31, I-98166 Messina, Italy
[g] Department of Health Sciences, University of Catanzaro "Magna Græcia", Campus Universitario "S. Venuta", Viale S. Venuta, Germaneto, I-88100 Catanzaro, Italy

ARTICLE INFO

Keywords:
Cyclodextrins
Inclusion complex
Drug delivery systems
Testosterone propionate
Physicochemical characterization

ABSTRACT

Hydroxypropyl-β-cyclodextrin (HP-β-CyD) and sulfobutyl ether-β-cyclodextrin (SBE-β-CyD) were used to generate hydrophilic complexes of the poorly water-soluble drug testosterone propionate (TP). The inclusion complexes were obtained by freeze-drying, and then analyzed at both liquid and solid states. Phase solubility studies, performed according to the type-A_L solubility diagrams of TP in presence of both CyDs, suggested the formation of water-soluble complexes at 1:1 molar ratio. These results were confirmed by continuous variation method (Job's plot). Both CyDs increased water-solubility of TP 100-fold as compared to the native drug. The *host-guest* arrangement of CyD complexes in a water solution was further investigated by one- and two-dimensional NMR spectroscopy, highlighting the insertion of the tetracyclic ring of TP into the CyD cavity, and the interaction of the pending ester chain of drug with the primary hydroxyl groups of CyDs at the narrow end of the toroid structure. In solid phase, FTIR-ATR spectroscopy showed that the C=O stretching mode of the TP vibrational spectrum changed if the complex between the drug and CyDs occurred. This change is temperature-dependent, and its evolution, accounted for by deconvolution procedures, provided the thermodynamic parameters explaining the mechanisms involved in the formation of inclusion complexes.

1. Introduction

Testosterone is the main sexual hormone produced by male testes. It plays a crucial role in the maintenance of basal fertility in men, and sexual behavior. A decrease in testosterone serum levels occurs with aging (Feldman et al., 2002; Harman et al., 2001) or hypogonadism (Stanworth and Jones, 2008). Low testosterone levels in men have shown to be linked to a decrease in quality of life, loss of libido and sexual performance, erectile dysfunction, and lack of energy (Khera, 2016a). Furthermore, other changes, such as loss of lean muscle mass, osteoporosis, depression, and depressed mood, have been reported (Giagulli et al., 2016). Testosterone replacement therapy represents the standard of care to restore hormone levels in serum, and decreases symptoms of hypogonadism. However, patients with hypogonadism and prostate cancer cannot receive an exogenous administration of testosterone formulations (American Association of Clinical Endocrinologists, 2002; Osterberg et al., 2014; Traish, 2016), since male's baseline testosterone levels may increase the progression of prostate cancer (Eisenberg, 2015; Siegel et al., 2017). The question is actually largely debated. Some studies report that high testosterone levels may decrease the incidence and progression of prostate cancer compared to low testosterone levels (Morgentaler and Rhoden, 2006). Other studies, however, showed that low testosterone levels significantly decrease prostate specific antigens and prevent the

* Corresponding authors.
E-mail addresses: vvenuti@unime.it (V. Venuti), caventura@unime.it (C.A. Ventura).

http://dx.doi.org/10.1016/j.ijpharm.2017.10.014
Received 2 August 2017; Received in revised form 5 October 2017; Accepted 9 October 2017
Available online 16 October 2017
0378-5173/

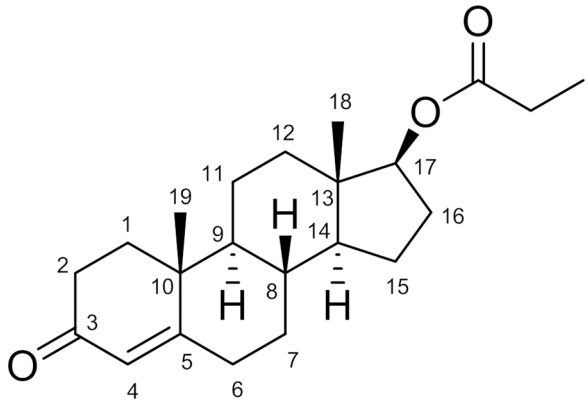

Fig. 1. Chemical structure of TP with assigned protons.

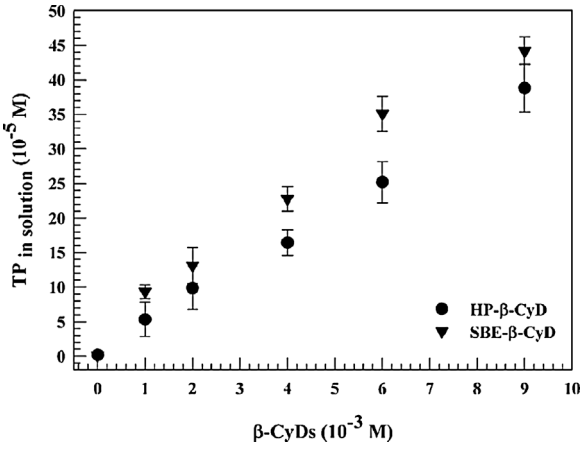

Fig. 2. Phase-solubility diagrams of TP by increasing the concentrations (0.0-9.0 mM) of SBE-β-CyD and HP-β-CyD in water at 25.0 ± 0.1 °C.

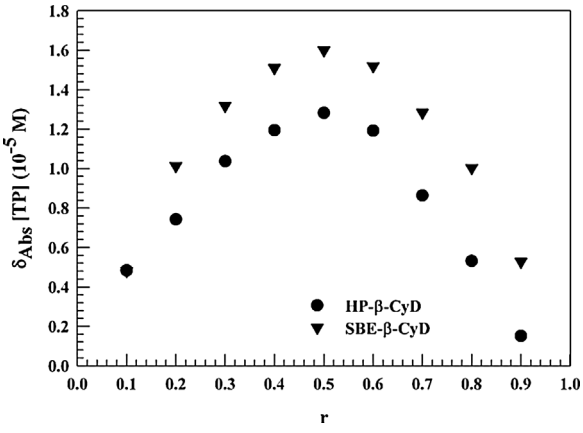

Fig. 3. Job's plot (continuous variation plot) for the complexation of TP with SBE-β-CyD and HP-β-CyD from absorbance measurements.

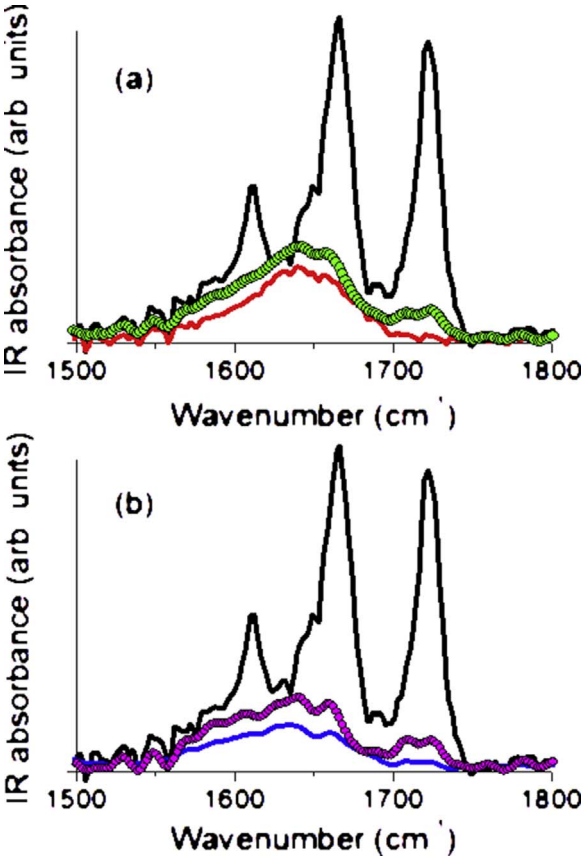

Fig. 4. (a) Experimental FTIR-ATR spectrum, at the 1500 ÷ 1800 cm^{-1} range and T = 300 K, of TP (black line), HP-β-CyD (red line), TP/HP-β-CyD inclusion complex (green circles). (b) Experimental FTIR-ATR spectrum, at the 1500 ÷ 1800 cm^{-1} range and T = 300 K, of TP (black line), SBE-β-CyD (blue line), TP/SBE-β-CyD inclusion complex (magenta circles). (For interpretation of the references to colour in this figure legend, the reader is referred to the web version of this article.)

recurrence and progression of prostate cancer in radical prostatectomy patients (Cornford et al., 2017; Morgentaler and Traish, 2009; Nguyen and Pastuszak, 2016; Morgentaler and Traish, 2009; Østergren et al., 2017; Salonia et al., 2013, 2012).

Testosterone and its long-acting hydrophobic derivatives are poor water soluble (0.005–0.039 mg/mL at 37 °C), and have a short plasma half-life of 10–20 min (British Pharmacopoeia, 1993), that can limit their use in experimental protocols and in clinics. Several testosterone drugs, including hepatotoxic oral formulations, transdermal patches, and gels are administered daily as a replacement therapy in patients with physiological or induced hormone deficiency (Hadgraft and Lane, 2015; Khera et al., 2016; Khera, 2016b; Srinivas-Shankar and Wu, 2006). The only injectable testosterone drug is marketed as an intramuscular oil-based depot formulation (Harle et al., 2005; Hohl et al., 2009), which needs multiple daily injections, is associated to adverse side effects and linked to poor patient compliance. Alternative formulations to improve testosterone delivery are needed.

Solubilizers, such as cyclodextrins (CyDs), can increase the water solubility of lipophilic drugs, improving their bioavailability (Cannavà et al., 2013; Ferrati et al., 2015a; Kurkov and Loftsson, 2013; Ventura et al., 2001; Venuti et al., 2014). In particular, hydroxypropyl-β-CyD (HP-β-CyD) and sulfobutylether-β-CyD (SBE-β-CyD) generate stronger complexes with hydrophobic molecules than the parent CyDs, without providing any cytoxicity associated with β-CyD (Gould and Scott, 2005; Stella and He, 2008). Also, HP-β-CyD and SBE-β-CyD are FDA approved as injectable products for intramuscular (i.m.) or intravenous (i.v.) administrations (Brewster and Loftsson, 2007). It has been demonstrated that HP-β-CyD and SBE-β-CyD can control testosterone release from simulated osmotic pump tablets (Okimoto et al., 1999) or nanochannel implant systems (Ferrati et al., 2015b). CyDs based testosterone complexes were formulated, as sublingual tablets, and studied by Salehian et al. (1995) as a hormone replacement therapy for young adolescents with delayed puberty deficits, and elderly men affected by androgen deficiency. Other data (Stuenkel et al., 1991) showed that the HP-β-CyD-testosterone complex was rapidly absorbed by the sublingual route, and quickly metabolized without increasing dihydrotestosterone or estradiol systemic metabolites. Although, HP-β-CyD-testosterone has been previously described as a potential therapeutic agent (Ferrati et al., 2015b; Okimoto et al., 1999), to the best of our knowledge, no

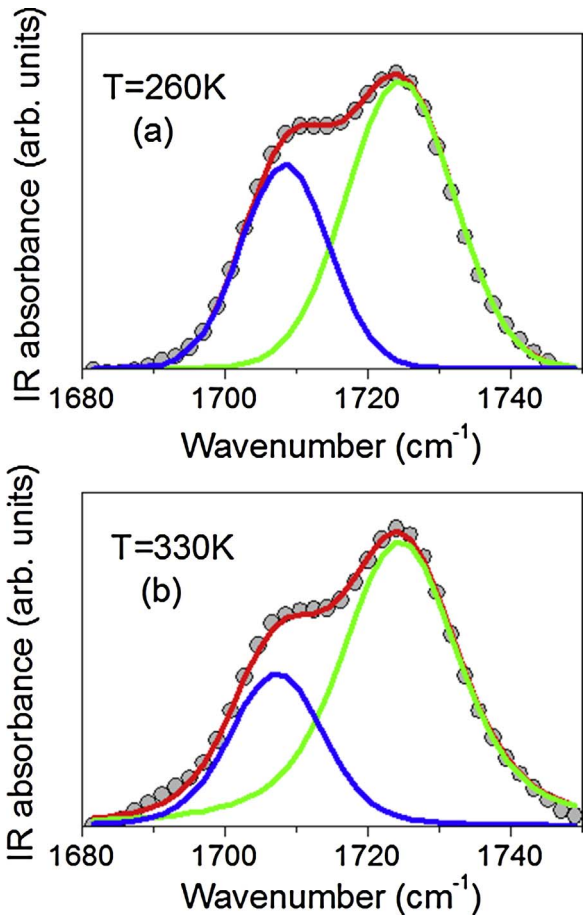

Fig. 5. Best-fit of the C=O stretching wavenumber range, for the TP/HP-β-CyD inclusion complex, at (a) T = 260 K and (b) T = 330 K, respectively. Experimental profile: grey circles, total fit: red line, ω_1 component: blue line, ω_2 component: green line. Check the main text for details. (For interpretation of the references to colour in this figure legend, the reader is referred to the web version of this article.)

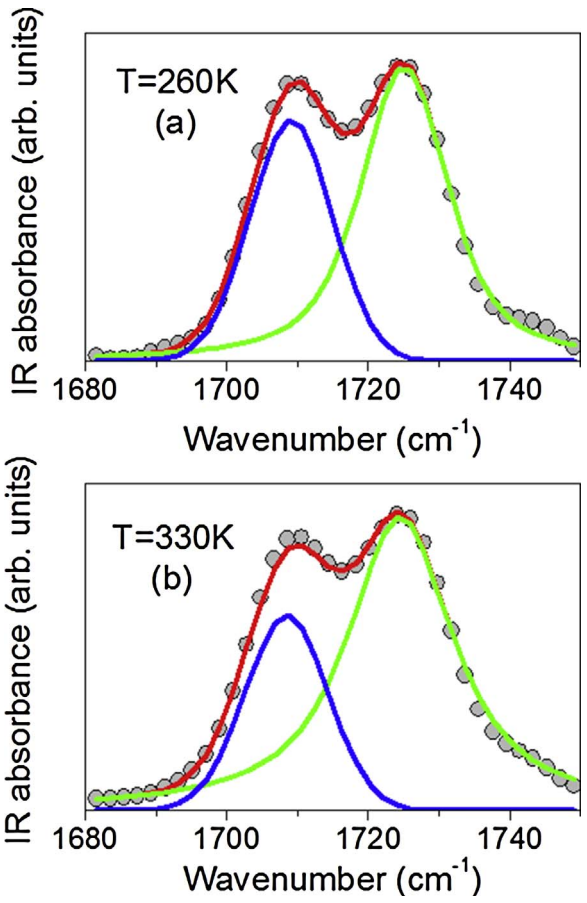

Fig. 6. Best-fit of the C=O stretching wavenumber range, for the TP/SBE-β-CyD inclusion complex, at (a) T = 260 K and (b) T = 330 K, respectively. Experimental profile: grey circles, total fit: red line, ω_1 component: blue line, ω_2 component: green line. Check the main text for details. (For interpretation of the references to colour in this figure legend, the reader is referred to the web version of this article.)

physicochemical analysis of the complex is available in literature.

In this study, we developed water-soluble formulations of testosterone based on CyDs complexation and performed a thorough physicochemical characterization of the compounds in view of their potential use as injectable formulations. Testosterone propionate (TP, Fig. 1) complexes with HP-β-CyD and SBE-β-CyD, and the stoichiometry of the inclusion complexes were tested in solution through phase-solubility analysis and Job's plot. One- and two-dimensional nuclear magnetic resonance (NMR) spectroscopy was used to investigate the *host-guest* interaction and the spatial disposition of TP into the inclusion complexes. The Fourier transform infrared spectroscopy in attenuated total reflectance geometry (FTIR-ATR) was applied to TP complexes with HP-β-CyD or SBE-β-CyD at solid state to study the *host-guest* interactions.

2. Materials and methods

2.1. Materials

Testosterone propionate (TP, $C_{22}H_{32}O_3$, MW 344.49) was purchased from Sigma-Aldrich (Milan, Italy). Hydroxypropyl-β-cyclodextrin (HP-β-CyD, with 0.6 molar substitution, average MW = 1380 g/mol) was kindly provided by Sigma-Aldrich (Milan, Italy). Sulfobutylether-β-cyclodextrin sodium salts (SBE-β-CyD, average degree of sulfobutyl substitutions of 7, average MW = 2162 g/mol) was kindly supplied by CyDex Pharmaceutical (Lenexa, Kansas City, USA). HP-β-CyD and/or SBE-β-CyD were used without any further purification. Double-distilled and deionized water was filtered through 0.22 μm Millipore® GSWP filters (Bedford, USA), and used for the analysis. All other chemicals and solvents were of analytical grade and obtained from Sigma-Aldrich (Milan, Italy).

2.2. Preparation of inclusion complexes

The inclusion complexes between TP and CyDs, namely SBE-β-CyD and HP-β-CyD, were prepared at 1:1.5 and 1:2 molar ratios, respectively, using the freeze-drying method. Briefly, SBE-β-CyD (945 mg) or HP-β-CyD (805 mg) was dissolved in 80 mL of water at room temperature, and added to a methanol solution (20 mL) containing TP (100 mg). The resulting solutions were stirred for 30 min, in the absence of light and at room temperature, and then subjected to a freeze-drying process (VirTis Gardiner, USA BenchTop K Series Freeze Dryers). All samples were divided into freeze-drying flasks and placed into the vacuum chamber, frozen at − 40 °C, and then freeze dried for 72 h.

2.3. Water solubility of native TP and resulting CyD complexes

The water solubility of free TP and TP/SBE-β-CyD or TP/HP-β-CyD inclusion complexes was quantified by suspending the drug in 3 mL of water, and stirring at 25.0 ± 0.1 °C for 24 h. The suspensions were then filtered through Sartorius Minisart®-SRP 15 PTFE 0.22 μm filters (Germany) and analyzed by UV–vis spectroscopy (FullTech Instruments, Rome, Italy) with a double beam spectrophotometer mod. PG T80. Quartz cuvette (1 cm path length, Hellma, Milan, Italy) were used in the 200 ÷ 400 nm spectral range. All measurements were carried out at 25.0 ± 0.1 °C. All data are the average of at least three

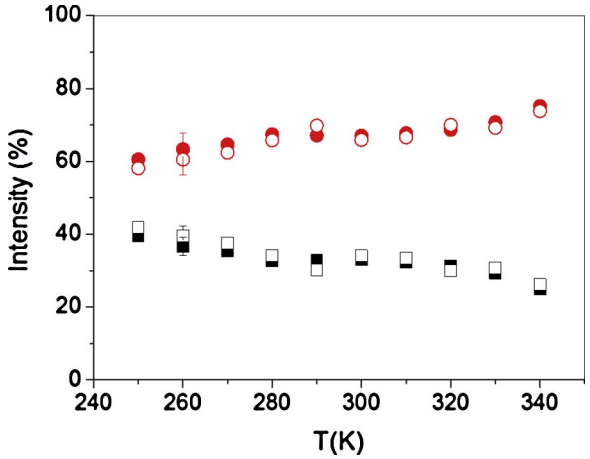

Fig. 7. Temperature evolution of the percentage intensities of the C=O stretching contributions of complexed (I_1: squares) and uncomplexed (I_2: circles) TP molecules in the TP/HP-β-CyD (closed symbols) and the TP/SBE-β-CyD (open symbols) inclusion complexes.

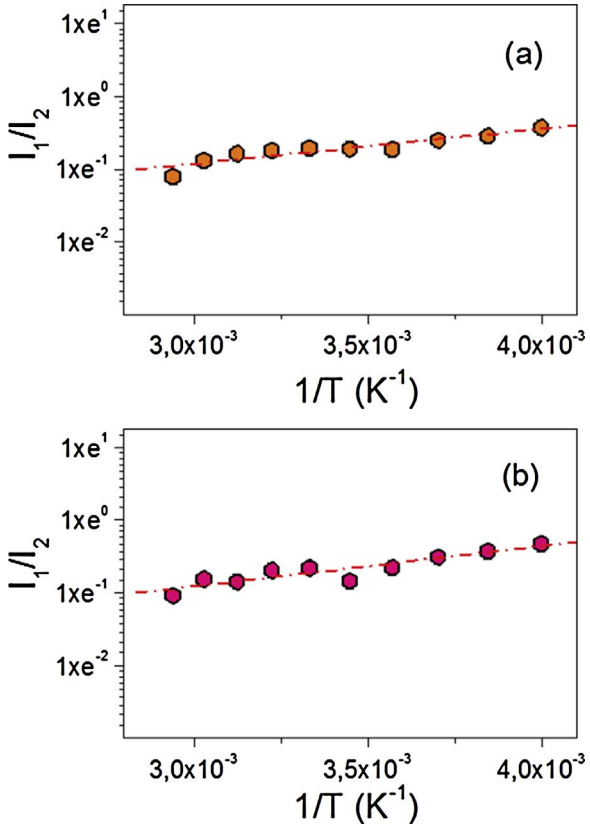

Fig. 8. Trends, as a function of 1/T, expressed as a semi-log plot, of I_1/I_2 for (a) the TP/HP-β-CyD and (b) the TP/SBE-β-CyD complexes. Red lines represent the best fit obtained according to Eq. (2). (For interpretation of the references to colour in this figure legend, the reader is referred to the web version of this article.)

independent measurements.

2.4. Phase-solubility analysis

An excess of TP, over drug solubility, was added to the aqueous solutions of SBE-β-CyD or HP-β-CyD (0.0-9.0 mM) into the 10 mL plastic tubes, and then sonicated using a water bath sonicator (Bandelin RK 514, Berlin, Germany) for 15 min. Flasks were sealed and then stirred in a Telesystem magnetic stirring bath warmed at 25.0 ± 0.1 °C with a Telemodul 40 °C control unit. After 24 h of incubation, the resulting suspensions were filtered through Sartorius Minisart®-SRP 15 PTFE 0.22 µm filters, samples (2 mL) were withdrawn, diluted, and assayed using a UV–vis spectrophotometer (245 nm) to measure the amount of TP dissolved in the water solution. Experiments were carried out in triplicate, and the resulting solubility data were averaged and further used to calculate the binding constant of TP/SBE-β-CyD and TP/HP-β-CyD complexes. The Higuchi and Connors (1965) equation was applied to calculate this parameter, as reported (Eq. (1)):

$$K_c = \frac{\alpha}{S_0 \cdot (1 - \alpha)} \quad (1)$$

where, α is the slope of the linear plot showing the amount of TP and CyD forming the complexes as a function of the CyD amount added during the preparation procedure, and S_0 is the solubility of TP in water.

2.5. Continuous variation method

Equimolar ($6 \cdot 10^{-5}$ M) methanol/water solutions (55/45, v/v) of TP and SBE-β-CyD or HP-β-CyD were mixed to a fixed volume varying the molar ratio from 0.1 to 0.9, and keeping the final molar concentration of both compounds constant. After 1 h of incubation, absorbance of the resulting solution was measured using UV–vis spectroscopy at 245 nm, and the ΔAbs was determined as the difference between the Abs with and without CyD.

ΔAbs × [TP] was plotted versus R (R = [TP]/[TP] + [HP-β-CyD] and [TP]/[TP] + [SBE-β-Cyd], respectively) (Tablet et al., 2012).

2.6. FTIR-ATR spectroscopy

Fourier transform infrared spectroscopy (FTIR) measurements in attenuated total reflectance (ATR) geometry were carried out on solid samples, at the 600 ÷ 4000 cm^{-1} wavenumber range, in the 250 K ÷ 340 K temperature range. Spectra were recorded using a Bomem DA8 Fourier transform spectrometer operating with a Globar source, in combination with a KBr beam splitter, and a thermoelectrically cooled deuterated triglycene sulphate (DTGS) detector. The powders were held in the Golden Gate diamond ATR system, based on the ATR technique. Data were collected in dry atmosphere, with a resolution of 4 cm^{-1}, automatically adding 100 repetitive scans to achieve good signal-to-noise ratio and high reproducibility. All FTIR-ATR spectra were normalized for taking the effective number of absorbers into account. No mathematical corrections (e.g. smoothing) were applied, while baseline adjustment and normalization were performed using a Spectracalc software package GRAMS (Galactic Industries, Salem, NH, USA). Band deconvolution of the 1500 ÷ 1800 cm^{-1} region, where the C=O stretching vibrational mode typically falls, was performed by means of second derivative computations, which were used to evaluate wavenumbers of the maxima of the different sub-bands. Based on these results, a multiple curve fitting routine provided in the PeakFit 4.0 software was then applied to the experimental profiles. Specifically, Voigt fitting functions were selected, and all parameters freely varied upon iteration. For each fitting session, multiple iterations were performed until a converging solution was reached by minimization of the value of χ^2. The procedure used allows applying the minimum number of parameters during analysis. The best fit is characterized by a $\chi^2 \cong 0.9999$ for all sets of samples.

2.7. NMR spectroscopy

NMR spectra were recorded on a Varian 500 MHz spectrometer at 25 °C in a 1:1 (v/v) D_2O:CD_3OD mixture. Chemical shifts (δ) are expressed in ppm. Two-dimensional ROESY experiments were performed using Varian standard pulse sequences.

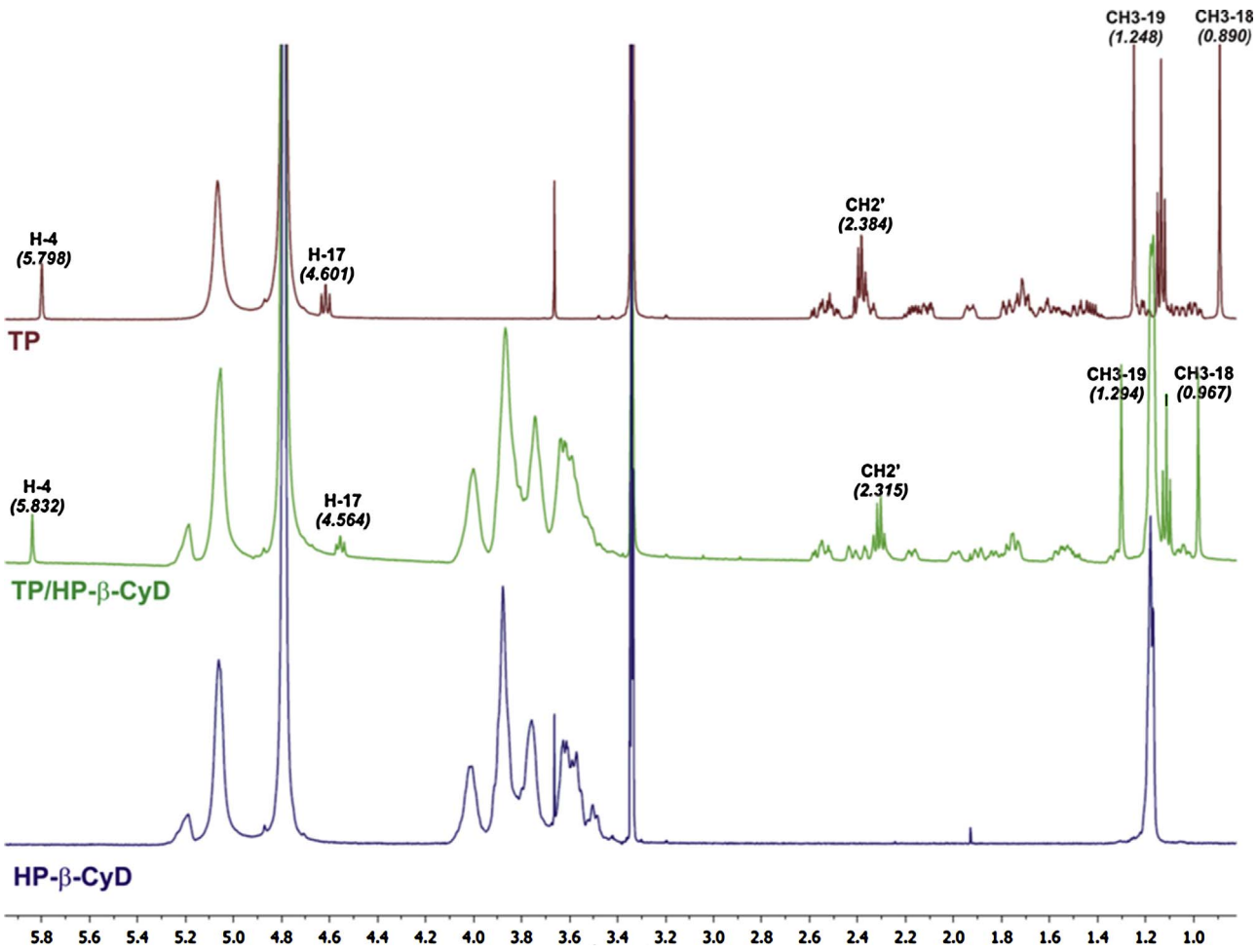

Fig. 9. ^{1}H NMR spectra of TP, TP/HP-β-CyDs and HP-β-CyDs. The chemical shifts (ppm) of the signals, showing the most significant shift displacements, are reported.

3. Results and discussion

TP/SBE-β-CyD and TP/HP-β-CyD complexes were obtained by freeze-drying at 1:1.5 and 1:2 molar ratios, respectively. TP is poor water-soluble (0.0056 mg/mL) at 25 °C and its resulting complex with the CyDs increased water solubility by ~100-fold (0.5771 mg/mL and 0.5521 mg/mL for TP/SBE-β-CyD and TP/HP-β-CyD complexes, respectively). Phase-solubility studies of the complexes were carried out to evaluate the *host-guest* interaction between TP and CyDs. The resulting isotherms showed a linear increase (A_L type curve) of TP water solubility by increasing the amount of both CyDs, and a slope below 1 (Fig. 2). These data demonstrated that a 1:1 stoichiometry of complexes between TP and SBE-β-CyD or HP-β-CyD was obtained over the full range of CyD concentration during analysis. The stability constants (Kc) of TP/SBE-β-CyD and TP/HP-β-CyD complexes were calculated using phase-solubility diagrams, according to the Higuchi and Connors (1965) equation, and the results were 55053 M^{-1} (TP/SBE-β-CyD) and 42938 M^{-1} (TP/HP-β-CyD).

The 1:1 stoichiometry of complexes between TP and SBE-β-CyD or HP-β-CyD was in agreement with Job's plot (continuous variation method) of resulting curves, which showed high symmetrical shape of the peak, and a maximum value at r = 0.5 for both complexes (Fig. 3).

3.1. FTIR-ATR spectroscopy

Fig. 4 shows the experimental FTIR-ATR spectra, at the 1500 ÷ 1800 cm^{-1} range, at T = 300 K as example, of uncomplexed TP, the macrocycles, and the corresponding 1:1 inclusion complexes.

The choice of this wavenumber range is justified by the appearance, at ~1723 cm^{-1}, of the C═O stretching band of the TP, which was strongly IR-active and did not overlap the strong absorption bands of CyDs. As a consequence, the C═O stretching band can represent an excellent marker to trace modifications of the complexes due to the activation of *host-guest* interactions.

A new C═O stretching vibrational peak at ~1705 cm^{-1} appeared for TP/HP-β-CyD and TP/SBE-β-CyD complexes. This peak was indicative of the involvement of this functional group in the activation of some *host-guest* interactions between TP and HP-β-CyD or SBE-β-CyD. This effect enforced the electrostatic environment surrounding the C═O group, while the carbonyl double bond weakened, and its stretching frequency moved towards lower values. Moreover, the C═O stretching signal of the free TP is still well distinguishable in the spectra of inclusion complexes, thus showing that a portion of the TP molecules did not make a complex with CyDs.

The peaks at ~1611 cm^{-1} and ~1655 cm^{-1} of free TP corresponded to the C–C and C═C stretching vibrations of the aromatic ring of the TP. These peaks cannot be detected in the spectra of the inclusion complexes, since they almost completely overlap with the δ_{HOH} bending band, at ~1640 cm^{-1}, derived from the crystallization water molecules of CyDs. As a consequence, no hypothesis can be made on eventual modifications they underwent upon complexation process. Furthermore, as the δ_{HOH} bending mode is due to those H_2O molecules not involved in tetrahedral environments (Brubach et al., 2005), its observation in the spectra of inclusion complexes suggests the presence of water molecules, probably in molecular form, considering the hydrophobic nature of the CyD cavities, even after inclusion.

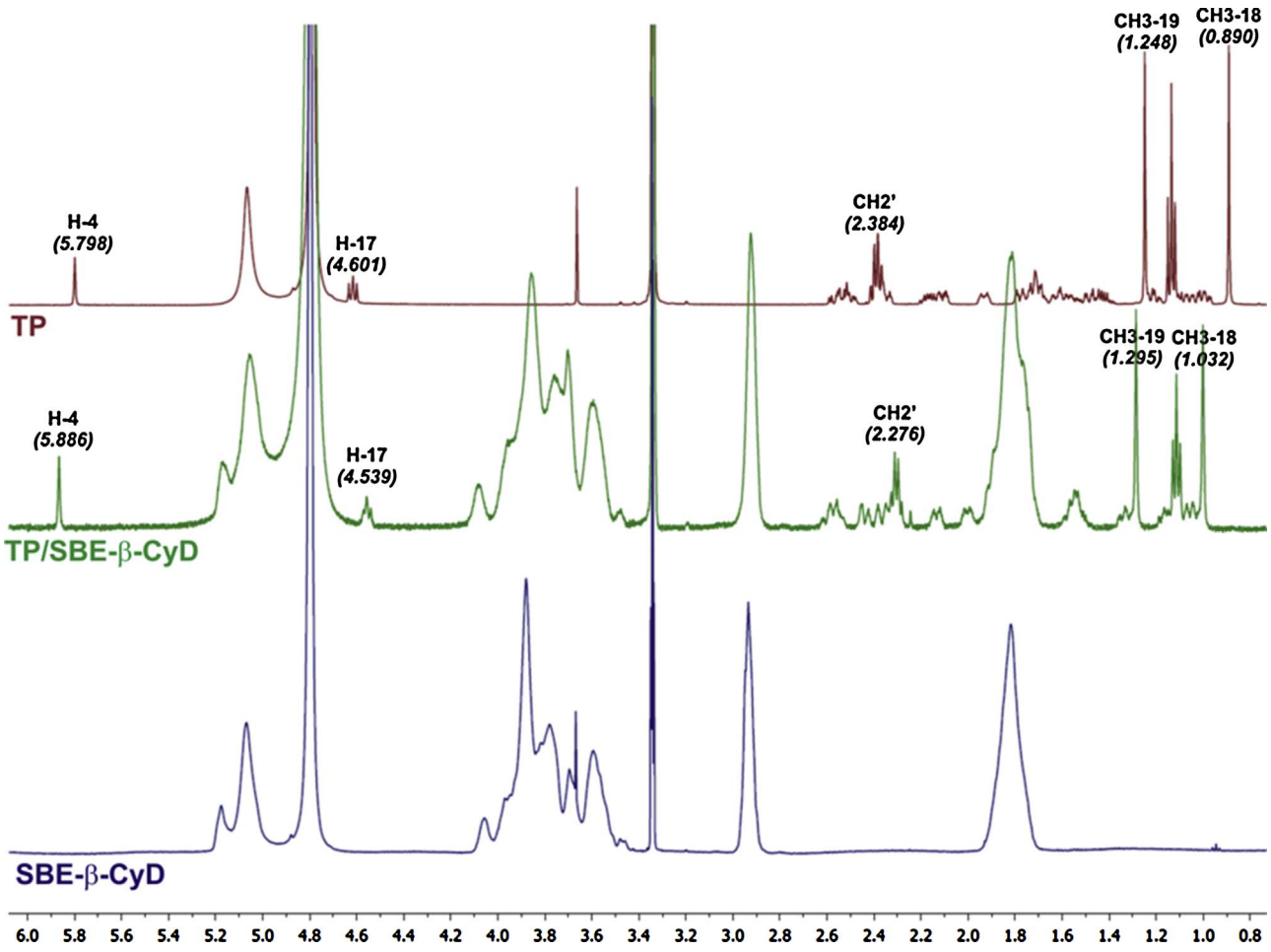

Fig. 10. ^{1}H NMR spectra of TP, TP/SBE-β-CyDs and SBE-β-CyDs. The chemical shifts (ppm) of the signals, showing the most significant shift displacements, are reported.

With the aim of performing a quantitative analysis of the different vibrational contributions concurring to the stretching vibration of carbonyl groups, a curve-fitting of the 1500 ÷ 1800 cm^{-1} region was operated.

The three minima observed, at ~1640 cm^{-1}, ~1705 cm^{-1} and ~1723 cm^{-1} respectively, in second derivative profile of the experimental spectra (data not shown) of TP/HP-β-CyD and TP/SBE-β-CyD complexes were used as starting values of the maxima of each sub-band in the spectrum itself. Based on the comparison between the FTIR-ATR spectra of free TP and TP/CyDs inclusion complexes, the first component comes from the δ_{HOH} bending of water molecules, whereas the other two contributions respectively reflect the C═O stretching mode of TP molecules that made or did not make a complex with CyDs.

The δ_{HOH} bending contribution was further subtracted from the spectra of TP/CyD complexes, and a second, more detailed, fitting procedure was then operated only for the carbonyl stretching vibration. Finally, two classes of C═O oscillators, stretching at ω_1 ~ 1705 cm^{-1} (TP making complexes with CyDs) and ω_2 ~ 1723 cm^{-1} (TP that did not make complexes with CyDs) respectively, are needed to reproduce the experimental spectra in a reliable way. Figs. 5 and 6 shows the results of the best-fit procedure, at T = 260 K and T = 330 K as examples, for TP/HP-β-CyD and TP/SBE-β-CyD, respectively.

Fig. 7 reports the temperature behavior of percentage intensities, I_1 and I_2 respectively, of ω_1 and ω_2 C═O sub-bands.

By following a well-established approach, already successfully applied in a variety of similar systems (Crupi et al., 2010, 2011), the behavior vs. T of $\frac{I_1}{I_2} = \frac{n_1}{n_2}$ (*n* being the number of oscillators involved in a specific IR vibration of intensity *I*), is found to obey the following law:

$$\ln\frac{I_1}{I_2} = -\frac{\Delta H}{RT} + \frac{\Delta S}{R}. \quad (2)$$

In the above expression, *R* represents the gas constant, ΔH and ΔS are, respectively, the enthalpy and entropy changes due to the establishment of host-guest interactions of the analyzed 1:1 inclusion complexes in solid state.

The best-fit results are reported in Fig. 8(a) and (b) for TP/HP-β-CyD and TP/SBE-β-CyD, respectively.

From the linear fit expressed in Eq. (2) we obtained $\Delta H = -4002 \pm 591$ J mol^{-1} for the TP/HP-b-CyD inclusion complex, and $\Delta H = -4625 \pm 703$ J mol^{-1} for the TP/SBE-β-CyD inclusion complex, respectively.

These values are comparable, revealing a similar mechanism driving the complexation process of TP in both cases. Furthermore, the large, negative values of ΔH might suggest the release of crystallization H_2O molecules from the hydrophobic cavity of CyDs and their replacement with TP molecules, less polar than water, with a consequent diminishing of the total enthalpy of the system. In solid state, SBE-β-CyD is shown to give rise to a slightly more stable inclusion complex, in agreement with what is revealed, in liquid state, by phase solubility analysis results.

3.2. NMR spectroscopy

The *host-guest* interaction between TP and CyDs in the liquid state was investigated by NMR spectroscopy using a 1:1 (v/v) D_2O/CD_3OD mixture.

The ^{1}H NMR spectra showed a shift of the proton signals of TP for

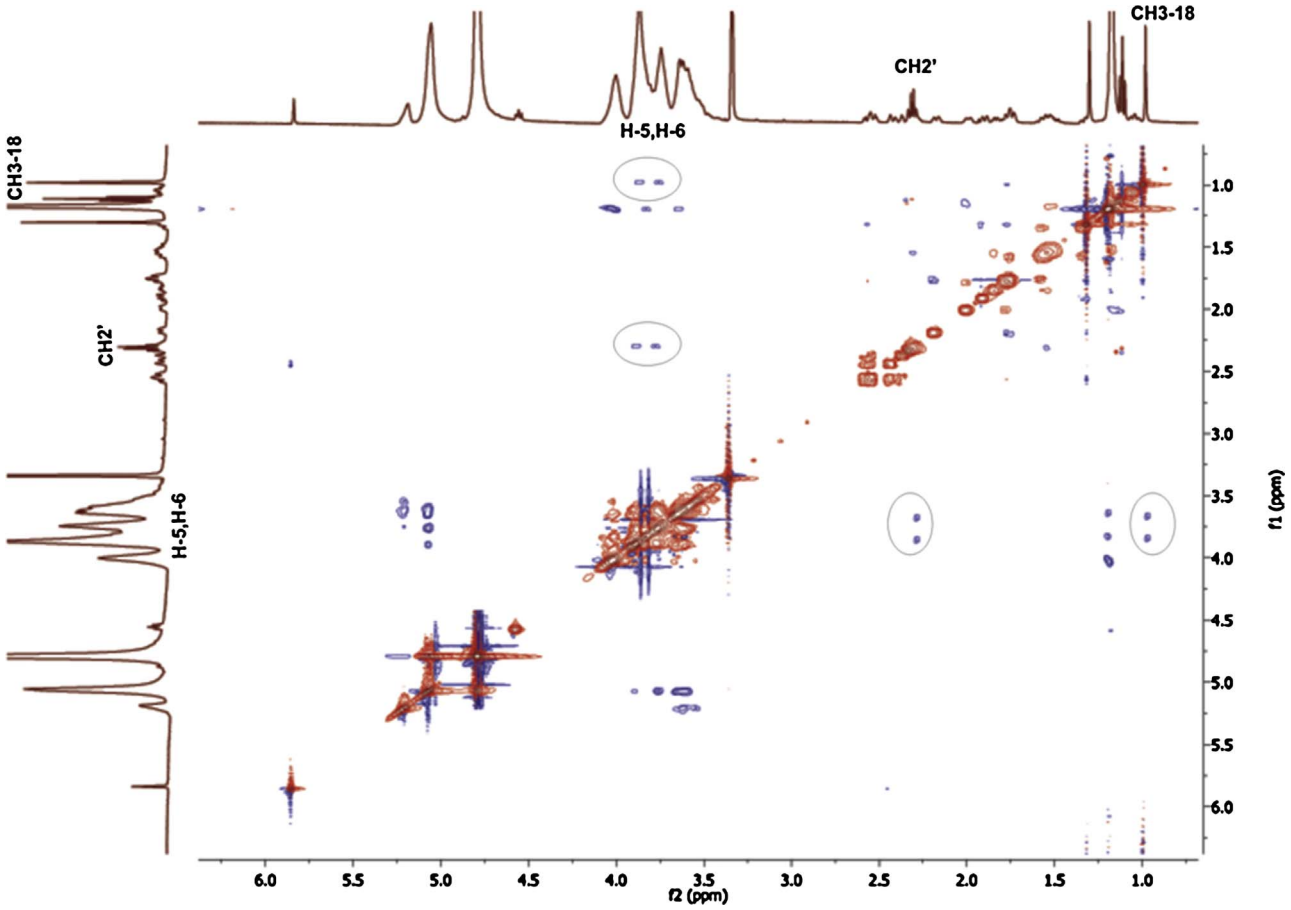

Fig. 11. ROESY spectrum of the TP/HP-β-CyDs. The cross peaks between CH3-18 (TP), CH2′ (TP) and H-5, H-6 (CyDs) are black-circled.

the TP/HP-β-CyD (Fig. 9) and TP/SBE-β-CyD (Fig. 10) inclusion complexes, compared to the free drug, whereas no detectable shifts of the signals of the CyDs were registered, likely because they are typically fairly broad. Moreover, specific modifications in the pattern of the signals of the TP protons in the aliphatic region (0.8–2.6 ppm) were obtained for both the inclusion complexes compared to the free TP. These changes depended on a specific interaction between the drug and the CyDs. In particular, the up-field shift of the protons of guest molecules shows that they are confined to the electronegative atom, such as oxygen; while the downfield shift of the protons depends on the inclusion of the drug inside the hydrophobic cavity of CyDs. This phenomenon provides a modification of the local polarity (Ganza-Gonzalez et al., 1994). In particular, the protons CH_3-18, CH_3-19 and H-4 of TP showed a down-field displacement for both the TP/HP-β-CyD (Fig. 9) and TP/SBE-β-CyD (Fig. 10) inclusion complexes, thus showing that the α, β-unsaturated carbonyl group, and the central portion of TP are included in the cavity of CyDs. Conversely, the proton H-17 and the CH_2 of the side ester chain of TP are up-field shifted, thus showing that they are closed to the oxygen atoms at the primary hydroxyl rim of the HP-β-CyD (Fig. 9), and SBE-β-CyD (Fig. 10).

The 2D-ROESY experiments showed the sites of interaction of TP with the HP-β-CyD or SBE-β-CyD. The geometry of *host-guest* inclusion complexes can be obtained by analyzing the interaction of the protons of the guest molecules with the H-3, H-5 and H-6 protons, lying on the internal (H-3, H-5) surface or surrounding the narrower rim (H-6) of CyDs cavity. The ROESY spectrum of the TP/HP-β-CyD (Fig. 11) showed the presence of cross-peaks between the protons H-5, H-6 of the HP-β-CyD and specific protons of TP (i.e. CH_3-18 and the CH_2 of the ester side chain). Similar results were obtained for the ROESY spectrum of the TP/SBE-β-CyD (Fig. 12). In both complexes, no cross-peaks of the TP proton signals were detected for the H-3 of the HP-β-CyD and SBE-β-CyD, respectively, thus showing that TP is deeply inserted into the cavity of the CyDs, as further confirmed by the interaction of TP with H-6 protons of CyDs at the narrow end of the toroid structure. NMR analysis demonstrated the inclusion of the tetracyclic ring of TP inside the hydrophobic cavity of the HP-β-CyD and SBE-β-CyD; conversely, the side ester chain of TP comes into contact with the primary hydroxyl groups (narrow rim) of CyDs, thus affecting the geometry of TP/HP-β-CyD, and TP/SBE-β-CyD complexes, respectively (Fig. 13).

4. Conclusions

The combined use of FTIR-ATR spectroscopy and 2D-ROESY experiments provided valuable information to explain the complexation mechanism and geometry of the inclusion complexes of TP with HP-β-CyD and SBE-β-CyD. In the solid phase, the presence of the *host-guest* interactions between TP and HP-β-CyD or SBE-β-CyD has been supposed through the spectral modifications of the specific bands of the guest which occurred upon making complexes. A quantitative analysis, as a function of temperature, was performed in the C═O stretching wavenumber range of the FTIR-ATR spectra of the TP/HP-β-CyD and TP/SBE-β-CyD inclusion complexes, according to a well-established model. As main result, it suggested an enthalpy-driven inclusion mechanism, furnishing the ΔH values associated to the binding between host and guest. The SBE-β-CyD provided a more stable inclusion complex with TP than HP-β-CyD. NMR analysis endorsed the formation of the inclusion complexes between TP and HP-β-CyD or SBE-β-CyD. In particular, ROESY analysis showed that the tetracyclic ring of TP was included inside the hydrophobic cavity of CyDs starting from their primary hydroxyl groups; while the side ester chain was exposed to the narrow rim of the CyDs. The resulting TP/HP-β-CyD and TP/SBE-β-CyD increased the water solubility (100-fold) of the drug, and made a stable

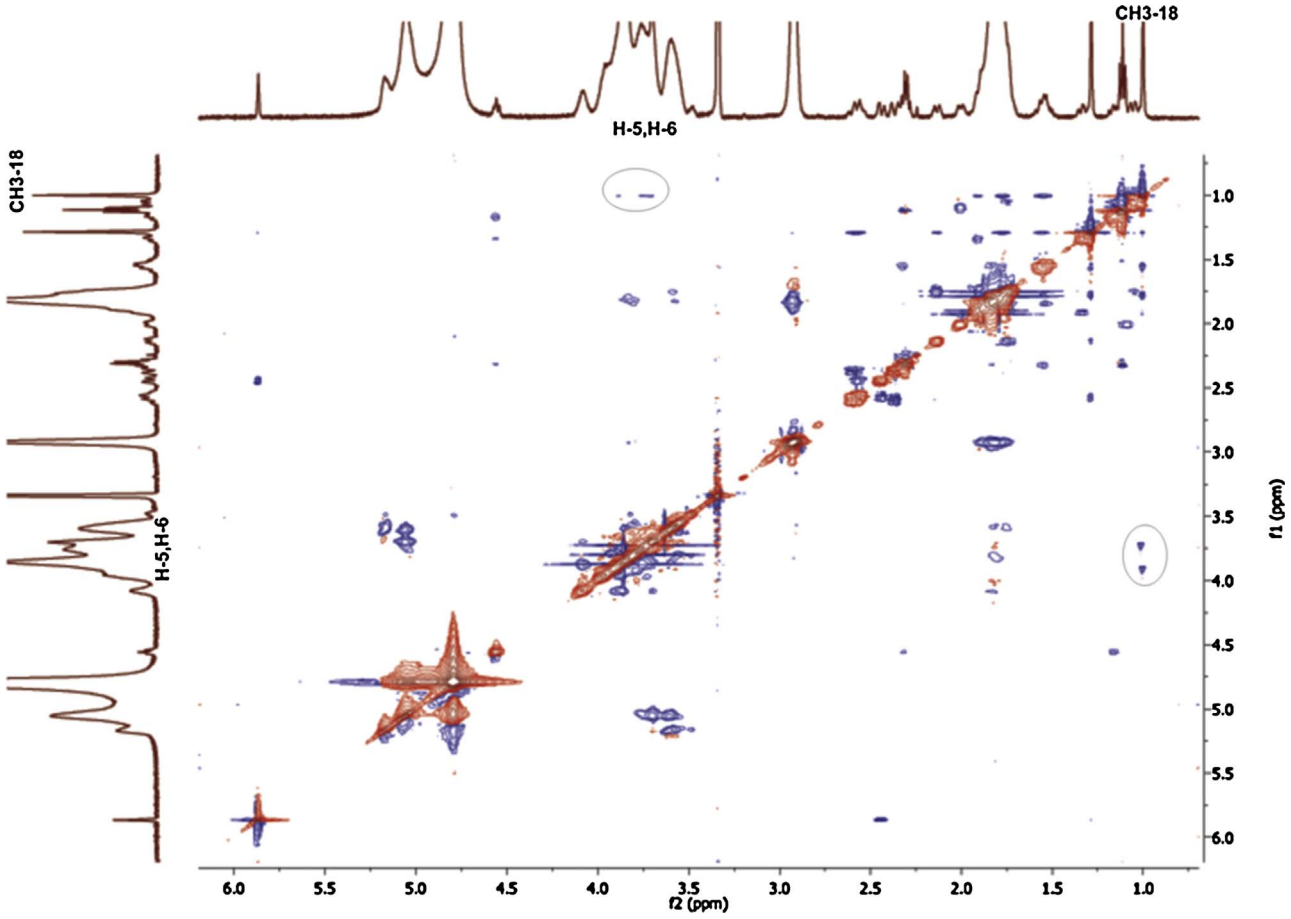

Fig. 12. ROESY spectrum of TP/SBE-β-CyDs. The cross peaks between CH3-18 (TP) and H-5, H-6 (CyD) are black-circled.

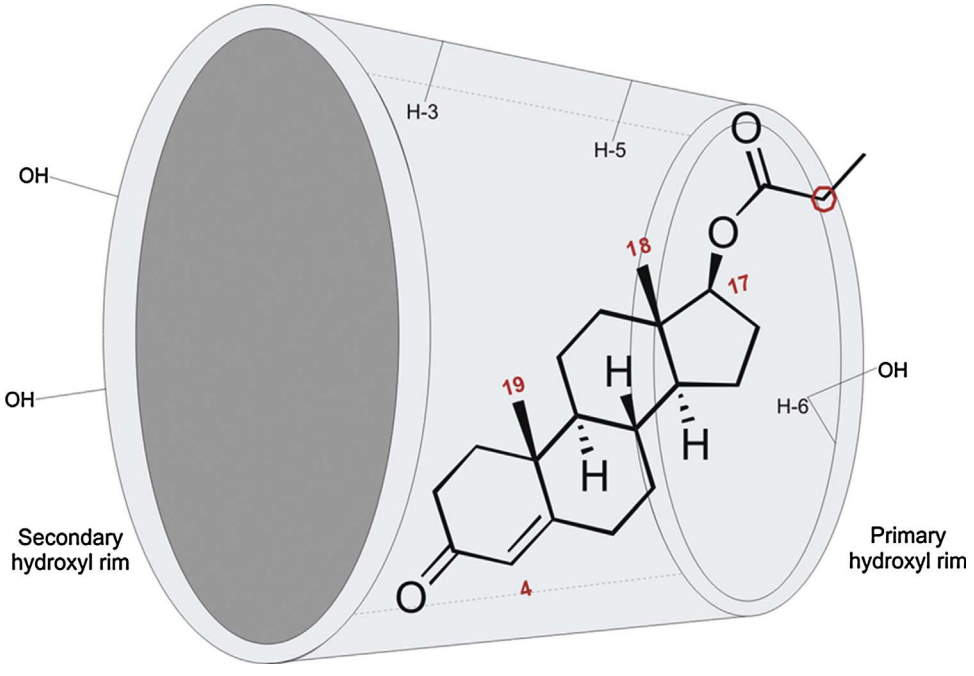

Fig. 13. Modeling of the structure showing the inclusion complex between TP and CyDs.

complex that was independent from the CyD derivatives. The resulting water soluble and stable complexes can be used as therapeutic payload in sustained release delivery devices, thus improving the clinical potential of TP in replacement hormone therapy or as an adjuvant in anticancer therapy.

Conflict of interest

The authors declare that they have no conflict of interest. We further agree with the policies on sharing data and materials, as reported in the guide for authors.

Author contributions

Vincenza Crupi (V. C.), Angela Scala (A. S.), Emanuela Surdo (E. S.) did experiments and acquired data.

Christian Celia (C. C.), Vincenza Crupi (V. C.), Massimo Fresta (M. F.), Alessandro Grattoni (A. G.), Domenico Majolino (D. M.), Nicola Micale (N. M.), Angela Scala (A. S.), Rosanna Stancanelli (R. S.), Silvana Tommasini (S. T.), Cinzia Anna Ventura (C. A. V.), Valentina Venuti (V. V.) critically revised the data.

Cinzia Anna Ventura (C.A.V.), Valentina Venuti (V. V.) designed the study and approved the final version of the manuscript before submission.

Acknowledgments

This work was financially supported by the Inter-Regional Research Center for Food Safety and Health (IRC-FSH) (grant no. PON a3_00359).

References

American Association of Clinical Endocrinologists, 2002. American Association of Clinical Endocrinologists medical guidelines for clinical practice for the evaluation and treatment of hypogonadism in adult male patients-2002 update. Endocr. Pract. 8, 439–456.

Brewster, M.E., Loftsson, T., 2007. Cyclodextrins as pharmaceutical solubilizers. Adv. Drug Deliv. Rev. 59, 645–666. http://dx.doi.org/10.1016/j.addr.2007.05.012.

Vol. I. British Pharmacopoeia Commission, London, 1993, pp. 654.

Brubach, J.B., Mermet, A., Filabozzi, A., Gerschel, A., Roy, P., 2005. Signatures of the hydrogen bonding in the infrared bands of water. J. Chem. Phys. 122, 184509. http://dx.doi.org/10.1063/1.1894929.

Cannavà, C., Crupi, V., Guardo, M., Majolino, D., Stancanelli, R., Tommasini, S., Ventura, C.A., Venuti, V., 2013. Phase solubility and FTIR-ATR studies of idebenone/sulfobutyl ether β-cyclodextrin inclusion complex. J. Incl. Phenom. Macrocycl. Chem. 75, 255–262. http://dx.doi.org/10.1007/s10847-012-0110-3.

Cornford, P., Bellmunt, J., Bolla, M., Briers, E., De Santis, M., Gross, T., Henry, A.M., Joniau, S., Lam, T.B., Mason, M.D., van der Poel, H.G., van der Kwast, T.H., Rouvière, O., Wiegel, T., Mottet, N., 2017. EAU-ESTRO-SIOG guidelines on prostate cancer. part II: treatment of relapsing, metastatic, and castration-resistant prostate cancer. Eur. Urol. 71, 630–642. http://dx.doi.org/10.1016/j.eururo.2016.08.002.

Crupi, V., Majolino, D., Venuti, V., Guella, G., Mancini, I., Rossi, B., Verrocchio, P., Viliani, G., Stancanelli, R., 2010. Temperature effect on the vibrational dynamics of cyclodextrin inclusion complexes: investigation by FTIR-ATR spectroscopy and numerical simulation. J. Phys. Chem. A 114, 6811–6817. http://dx.doi.org/10.1021/jp101888g.

Crupi, V., Guella, G., Majolino, D., Mancini, I., Paciaroni, A., Rossi, B., Venuti, V., Verrocchio, P., Viliani, G., 2011. Effect of the chiral discrimination on the vibrational properties of (R)-, (S)- and (R, S)-ibuprofen/methyl-beta-cyclodextrin inclusion complexes. Philos. Mag. 91, 1776–1785. http://dx.doi.org/10.1080/14786435.2010.512575.

Eisenberg, M.L., 2015. Testosterone replacement therapy and prostate cancer incidence. World J. Mens Health 33, 125–129. http://dx.doi.org/10.5534/wjmh.2015.33.3.125.

Feldman, H.A., Longcope, C., Derby, C.A., Johannes, C.B., Araujo, A.B., Coviello, A.D., Bremner, W.J., McKinlay, J.B., 2002. Age trends in the level of serum testosterone and other hormones in middle-aged men: longitudinal results from the Massachusetts male aging study. J. Clin. Endocrinol. Metab. 87, 589–598. http://dx.doi.org/10.1210/jcem.87.2.8201.

Ferrati, S., Nicolov, E., Bansal, S., Hosali, S., Landis, M., Grattoni, A., 2015a. Docetaxel/2-hydroxypropyl β-cyclodextrin inclusion complex increases docetaxel solubility and release from a nanochannel drug delivery system. Curr. Drug Targets 16, 1645–1649. http://dx.doi.org/10.2174/1389450116141511191255 41.

Ferrati, S., Nicolov, E., Bansal, S., Zabre, E., Geninatti, T., Ziemys, A., Hudson, L., Ferrari, M., Goodall, R., Khera, M., Palapattu, G., Grattoni, A., 2015b. Delivering enhanced testosterone replacement therapy through nanochannels. Adv. Healthc. Mater. 4, 446–451. http://dx.doi.org/10.1002/adhm.201400348.

Ganza-Gonzalez, A., Vila-Jato, J.L., Anguiano-Igea, S., Otero-Espinar, F.J., Blanco-Méndez, J., 1994. A proton nuclear magnetic resonance study of the inclusion complex of naproxen with β-cyclodextrin. Int. J. Pharm. 106, 179–185. http://dx.doi.org/10.1016/0378-5173(94)90001-9.

Giagulli, V.A., Guastamacchia, E., Licchelli, B., Triggiani, V., 2016. Serum testosterone and cognitive function in ageing male: updating the evidence. Recent Pat. Endocr. Metab. Immune Drug Discov. 10, 22–30. http://dx.doi.org/10.2174/1872214810999160603213743.

Gould, S., Scott, R.C., 2005. 2-Hydroxypropyl-β-cyclodextrin (HP-β-CD): a toxicology review. Food Chem. Toxicol. 43, 1451–1459. http://dx.doi.org/10.1016/j.fct.2005.03.007.

Hadgraft, J., Lane, M.E., 2015. Transdermal delivery of testosterone. Eur. J. Pharm. Biopharm. 92, 42–48. http://dx.doi.org/10.1016/j.ejpb.2015.02.015.

Harle, L., Basaria, S., Dobs, A.S., 2005. Nebido: a long-acting injectable testosterone for the treatment of male hypogonadism. Expert Opin. Pharmacother. 6, 1751–1759. http://dx.doi.org/10.1517/14656566.6.10.1751.

Harman, S.M., Metter, E.J., Tobin, J.D., Pearson, J., Blackman, M.R., 2001. Baltimore longitudinal study of aging. Longitudinal effects of aging on serum total and free testosterone levels in healthy men. J. Clin. Endocrinol. Metab. 86, 724–731. http://dx.doi.org/10.1210/jcem.86.2.7219.

Higuchi, T., Connors, K.A., 1965. Phase solubility techniques. Adv. Anal. Chem. Instrum. 4, 117–212.

Hohl, A., Marques, M.O., Coral, M.H., Walz, R., 2009. Evaluation of late-onset hypogonadism (andropause) treatment using three different formulations of injectable testosterone. Arq. Bras. Endocrinol. Metabol. 53, 989–995. http://dx.doi.org/10.1590/S0004-27302009000800013.

Khera, M., Adaikan, G., Buvat, J., Carrier, S., El-Meliegy, A., Hatzimouratidis, K., McCullough, A., Morgentaler, A., Torres, L.O., Salonia, A., 2016. Diagnosis and treatment of testosterone deficiency: recommendations from the fourth international consultation for sexual medicine (ICSM 2015). J. Sex Med. 13, 1787–1804. http://dx.doi.org/10.1016/j.jsxm.2016.10.009.

Khera, M., 2016a. Male hormones and men's qualities of life. Curr. Opin. Urol. 26, 152–157. http://dx.doi.org/10.1097/MOU.0000000000000256.

Khera, M., 2016b. Testosterone therapies. Urol. Clin. North Am. 43, 185–193. http://dx.doi.org/10.1016/j.ucl.2016.01.004.

Kurkov, S.V., Loftsson, T., 2013. Cyclodextrins. Int. J. Pharm. 453, 167–180. http://dx.doi.org/10.1016/j.ijpharm.2012.06.055.

Morgentaler, A., Rhoden, E.L., 2006. Prevalence of prostate cancer among hypogonadal men with prostate-specific antigen levels of 4.0 ng/mL or less. Urology 68, 1263–1267. http://dx.doi.org/10.1016/j.urology.2006.08.1058.

Morgentaler, A., Traish, A.M., 2009. Shifting the paradigm of testosterone and prostate cancer: the saturation model and the limits of androgen-dependent growth. Eur. Urol. 55, 310–320. http://dx.doi.org/10.1016/j.eururo.2008.09.024.

Nguyen, T.M., Pastuszak, A.W., 2016. Testosterone therapy among prostate cancer survivors. Sex Med. Rev. 4, 376–388. http://dx.doi.org/10.1016/j.sxmr.2016.06.005.

Okimoto, K., Rajewski, R.A., Stella, V.J., 1999. Release of testosterone from an osmotic pump tablet utilizing (SBE)7m-beta-cyclodextrin as both a solubilizing and an osmotic pump agent. J. Control. Release 58, 29–38. http://dx.doi.org/10.1016/S0168-3659(98)00142-4.

Osterberg, E.C., Bernie, A.M., Ramasamy, R., 2014. Risks of testosterone replacement therapy in men. Indian J. Urol. 30, 2–7. http://dx.doi.org/10.4103/0970-1591.124197.

Østergren, P.B., Kistorp, C., Fode, M., Henderson, J., Bennedbæk, F.N., Faber, J., Sønksen, J., 2017. Luteinizing hormone-releasing hormone agonists are superior to subcapsular orchiectomy in lowering testosterone levels of men with prostate cancer: results from a randomized clinical trial. J. Urol. 197, 1441–1447. http://dx.doi.org/10.1016/j.juro.2016.12.003.

Salehian, B., Wang, C., Alexander, G., Davidson, T., McDonald, V., Berman, N., Dudley, R.E., Ziel, F., Swerdloff, R.S., 1995. Pharmacokinetics, bioefficacy, and safety of sublingual testosterone cyclodextrin in hypogonadal men: comparison to testosterone enanthate–a clinical research center study. J. Clin. Endocrinol. Metab. 80, 3567–3575. http://dx.doi.org/10.1210/jcem.80.12.8530600.

Salonia, A., Abdollah, F., Capitanio, U., Suardi, N., Briganti, A., Gallina, A., Colombo, R., Ferrari, M., Castagna, G., Rigatti, P., Montorsi, F., 2012. Serum sex steroids depict a nonlinear u-shaped association with high-risk prostate cancer at radical prostatectomy. Clin. Cancer Res. 18, 3648–3657.

Salonia, A., Abdollah, F., Capitanio, U., Suardi, N., Gallina, A., Castagna, G., Clementi, M.C., Briganti, A., Rigatti, P., Montorsi, F., 2013. Circulating sex steroids and prostate cancer: introducing the time-dependency theory. World J. Urol. 31, 267–273. http://dx.doi.org/10.1007/s00345-012-1009-8.

Siegel, R.L., Miller, K.D., Jemal, A., 2017. Cancer statistics, 2017. CA Cancer J. Clin. 67, 7–30. http://dx.doi.org/10.3322/caac.21387.

Srinivas-Shankar, U., Wu, F.C., 2006. Drug insight: testosterone preparations. Nat. Clin. Pract. Urol. 3, 653–665. http://dx.doi.org/10.1038/ncpuro0650.

Stanworth, R.D., Jones, T.H., 2008. Testosterone for the aging male; current evidence and recommended practice. Clin. Interv. Aging 3, 25–44. http://dx.doi.org/10.2147/CIA.S190.

Stella, V.J., He, Q., 2008. Cyclodextrins. Toxicol. Pathol. 36, 30–42. http://dx.doi.org/10.1177/0192623307310945.

Stuenkel, C.A., Dudley, R.E., Yen, S.S.C., 1991. Sublingual administration of testosterone-hydroxypropyl-β-cyclodextrin inclusion complex simulates episodic androgen release in hypogonadal men. J. Clin. Endocrinol. Metab. 72, 1054–1059. http://dx.doi.org/10.1210/jcem-72-5-1054.

Tablet, C., Matei, J., Hillebrand, M., 2012. In: Innocenti, A. (Ed.), The Determination of the Stoichiometry of Cyclodextrin Inclusion Complexes by Spectral Methods: Possibilities and Limitations, Stoichiometry and Research – The Importance of Quantity in Biomedicine. InTech. ISBN: 978-953-51-0198-7, Available from: http://www.intechopen.com/books/stoichiometry-and-research-the-importance-ofquantity-in-biomedicine/-the-determination-of-the-stoichiometry-of-cyclodextrin-inclusion-complexes-byspectral-methods-poss.

Traish, A., 2016. Testosterone therapy in men with testosterone deficiency: are we beyond the point of no return? Investig. Clin. Urol. 57, 384–400. http://dx.doi.org/10.4111/icu.2016.57.6.384.

Ventura, C.A., Fresta, M., Paolino, D., Pedotti, S., Corsaro, A., Puglisi, G., 2001. Biomembrane model interaction and percutaneous absorption of papaverine through rat skin: effects of cyclodextrins as penetration enhancers. J. Drug Target. 9, 379–393.

Venuti, V., Cannavà, C., Cristiano, M.C., Fresta, M., Majolino, D., Paolino, D., Stancanelli, R., Tommasini, S., Ventura, C.A., 2014. A characterization study of resveratrol/sulfobutyl ether-β-cyclodextrin inclusion complex and in vitro anticancer activity. Colloids Surf. B 115, 22–28. http://dx.doi.org/10.1016/j.colsurfb.2013.11.025.